Journal of Simulation and Analysis of Novel Technologies in Mechanical Engineering
14 (4) (2022) 0025~0036

Research article

The effect of explosive welding variables on corrosion behavior of 304 stainless steel–copper joint in 3.5% NaCl solution concentration environment

Reza Peykari[1], Mohammad Reza Khanzadeh[*, 2], Hamid Bakhtiari[3]

[1]*Faculty of Materials Engineering, Islamic Azad University Shahreza Branch, Isfahan, Iran.*
[2]*Faculty of Engineering, Mobarakeh Branch, Islamic Azad University, Mobarakeh, Iran,*
[3]*Materials and Energy Research Center, Department of Ceramics, Karaj, Iran.*

[*]Khanzade@gmail.com

(Manuscript Received ---16 Nov. 2022; Revised --- 28 Dec. 2022; Accepted --- 29 Dec. 2022)

Abstract

In this study, the corrosion behavior and microstructural variations of two-layer sheets consisting of 304 stainless steel copper have been investigated after the explosive welding process. Explosive welding is carried out by variable explosive charges and changing the distance between the sheets. To investigate the corrosion behavior of the welding zone, dynamic potential polarization and electrochemical impedance imaging were used. Besides, to perform microstructural analysis, metallographic tests using an optical microscope and scanning electron microscope (SEM) were employed. In addition, micro-hardness is considered to investigate the effect of shock waves caused by the explosion. The results showed that the sample with an explosive thickness of 79 mm has the highest interface hardness (HV 549) due to the high thickness of the explosive layer and standoff distance (3 mm). Also, the polarization test results indicated that the lowest corrosion rate corresponds to the sample with an explosive charge thickness of 79 mm and a standoff distance of 2 mm, and the highest corrosion rate was related to the sample with a 46-mm explosive charge thickness and standoff distance of 3 mm. Based on the results obtained from the electrochemical impedance spectroscopy, It can be concluded that by increasing the amount of copper in the locally frozen melt of the samples, the intensity of corrosion caused by the galvanic cell increases.

Keywords: explosive welding, explosive charge thickness, intense plastic deformation, vortices

1- Introduction

Explosive welding is one of the solid-state welding processes. In this process, the explosive force hits the flying plate to the base plate at high speed, and as a result of applied pressure at the contact point, by creating pseudo-fluid behavior of metals and formation of the jet in the interface, the connection takes place. The most important variables in this welding process include the dynamic angle of collision, speed of collision point and flying plate, the collision pressure, standoff distance, and explosive charge. The explosive welding process can be used to connect multilayer metals, mainly to prevent corrosion, and improve the quality of heat transfer, resistance

to applied stresses, electrical properties, and surface abrasion properties. This process is used in industries such as power generation, construction of pressure vessels, heat exchangers, and shipbuilding industries [1-4]. A few studies have been conducted in the field of copper-to-steel explosive welding, as well as the corrosion of explosive connections. However, some of these studies are mentioned in the following paragraphs.

Yazdani et al. investigated the explosive welding of copper to stainless steel and indicated that with the increase of the flying plate thickness, the speed of the flying plate decreased, and with the increase of explosives thickness, a longer standoff distance is required to produce uniform explosive pressure [5]. Durgutlu et al. investigated the explosive welding of copper to stainless steel and indicated that the hardness profile near the interface was lower than the common hardness of the two flying and base plates, and the base plates which are caused by heat generated by the high-pressure contact and the annealing of the interface area. A medium hardness is achieved between two plates by local annealing in some common welding positions where hard work is involved [6]. Moreover, in the study of the effect of changing the parameters of the explosive load and the standoff distance in the explosive welding of copper-stainless steel, it was shown that with the increase of these variables, the shape of the interface changed from flat to wavy profile. Besides, the amplitude and length of waves increased at the interface. In addition, the hardness in the interface area and the outer surface of the sheets increased due to the deformation resulting from the collision of the plates. Besides, hardness enhancement in the interface increased with the increase of explosive charge and the standoff distance. With the increase of amplitude and length of waves in the interface, the interface tensile strength was enhanced due to the augmentation of the contact area [7]. In another study by Langeslag et al. on the effect of explosive charge on copper-steel welding, it was observed that with the increase of explosive load and contact pressure, wavelength and amplitude increased at the interface [8]. Kahraman et al. [9, 10] investigated the corrosion of explosive welding of Ti-6Al-4V and aluminum plates as well as titanium to stainless steel. Their results indicated that the increase of plastic deformation and explosive charge increased the weight loss in the corrosion test and led to the formation of an oxide layer on the surface. Kengkla and Tareelap [11] examined the corrosion behavior of explosive three-layer aluminum/steel connections. They indicated that the formation of intermetallic compounds at the interface provides a cathodic state relative to aluminum, and it caused an anodic state relative to steel. In addition, it provided selective corrosion near the aluminum boundary and intermetallic compounds. Acarer et al. [12] investigated the explosive welding of Al to copper. Their results showed that the galvanic corrosion occurred at the interface, and the aluminum side of the interface has a more significant anodic state based on a high electronegativity and was more corroded compared to the copper side. Moreover, Kamachi Mudali et al. [13] investigated the corrosion of a Titanium-304 stainless steel explosive welding. They indicated that the connection had an appropriate corrosion rate, and the higher corrosion rates were concentrated at the interface area. Investigating the effects of explosive material thickness and standoff distance on the corrosion properties of the explosive interface of stainless steel 304 using Dynamic Potential Polarization and Electrochemical Impedance Spectroscopy is a new and innovative problem that is investigated in the present research.

2- Experimental Method

2-1- Materials

In this research, copper and 304 stainless steel are considered as the flying plate and base plate respectively. The chemical composition of the alloys is listed in Table 1 [14]. The

metals were first cleaned and then cut into rectangular shapes of the following

Elements	Bal.	Sn%	Pb%	P%	Zn%	Si%	Ni%	Mn%	Cr%	Ti%
Copper	Cu	0.92	0.0123	0.0893	0.119	-	-	-	-	-
St.St 304	Fe	0.02	-	-	0.25	0.4	8	0.7	18	0.15

Steel base plate: 150 mm × 150 mm × 4 mm

Copper flying plate: 150 mm× 150 mm ×2mm

2-2- Explosive welding process

In this study, the heterogeneous connection between copper and 304 stainless steel was carried out by the explosive welding method. Fig. 1 shows the initial configuration of the plates for explosive welding. Flying and base plates are both designed in dimensions of 150 × 150 mm, and 95% Amatole explosive with a combination of 5% TNT, and 95% ammonium nitrate at 2507 m / s in the presence of an M8 detonator are used.

In order to establish the sheets to perform the explosive welding process, a concrete platform covered with sand bedding as a buffer and the interfaced layer was considered. In order to create the standoffs for each test, copper wires with appropriate diameters and the height of standoff distance were located between the 304 stainless steel and copper [14].

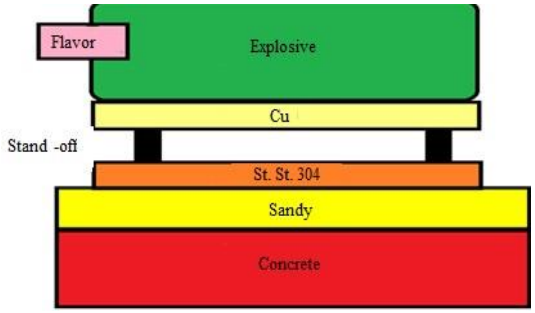

Fig. 1 the initial configuration of the plates for for explosive welding [14].

In Table 2, the parameters of explosive welding were determined in four parts. The standoff distance is set to 0.5 -1 times the flying plate width, and the thickness of the explosive is also selected so that the kinetic energy of the collision is sufficient.

Table 2: Variables of the welds performed [14]

Sample	standoff distance (mm)	Explosive Thickness (mm)
1	3	46
2	2	63
3	3	79
4	2	79

2-3- Tests

Samples of 10 × 10 mm were prepared. At first, small samples were cut using a wire cut device. The samples were cut perpendicular to the connection axis and the weld surface, and then the mounts were cooled. In order to prepare the samples for metallography, the surface of the samples was first sanded with SiC paper No. 60 to 2500. After removing the lines and surface roughness, they were polished with the device, felt and aluminum

oxide solution. Following this, the surface of the samples was washed and dried with alcohol, and then they were chemically engraved with 2% Nital solution. The microstructure of the interface was investigated by Olympus optical microscope in different magnifications. Besides, SEM with the capability of energy dispersive spectroscopy (EDS) made by VEGA Company was used for further investigations.

In order to investigate the corrosion behavior of explosive welding components in a 3.5% NaCl solution, a three-electrode electrothermal cell with a capacity of 500 ml was used for polarization and electrochemical impedance spectroscopy (EIS). An over-saturated calomel electrode (SCE) was used as a reference electrode, and platinum was used as an auxiliary electrode. All of the electrochemical experiments were conducted using the M1025 EG&G device manufactured by the United States and by the software Power suit 2.20.0. Dynamic Potential polarization experiments with the scan rate of 1 mV / s and initial potential of -250 mV lower than the open circuit potential to 250 mV above the open circuit potential were performed to determine the corrosion potential and current. The electrochemical impedance spectroscopy (EIS) test was conducted in the frequency range of 100 kHz to 10 MHz with an amplitude of 10 mV around the open circuit potential using the EG&G device of the M1025 constructed in the United States. The ZSimpWin 3.22 software package was used to analyze the EIS results. The time needed to reach a steady state is 90 minutes [15]. The surface of the test sample is very polished and roughened for micrographic studies. For doing this, the micro-hardness testing device is used. In this case, the applied force on the sample is 50 g for 10 seconds. Subsequently, the diameter is measured accurately according to the Vickers test method [16]. It should be noted that the hardness examination is carried out based on just the interface.

3- Results and discussion

3-1- Microstructure investigation of samples by optical microscope

Fig. 2a shows the waves created in the longitudinal direction of the joint. It can be observed that the interface in this mode is a short wave. This sample with a standoff distance of 3 mm and an explosive thickness of 46 mm is less than that of the second, third, and fourth series with a smaller wavelength range due to the thickness of the explosive. In explosive welding, two interfaces metal-to-metal and metal-to-solidified molten can be obtained. Along with the minimum speed of the flying plate, there is a minimum amount of collisional kinetic energy for the joint. As a result of the flying plate collision, the kinetic energy is converted into potential energy and leads to the deformation of the collision surface. If the amount of plastic deformation is not sufficient, short waves are created and the local melting zone does not appear. With the increase of kinetic energy, extreme deformation occurs at the bottom and crest of the wave. As a result of high collision pressures, the vortex can be formed at the interface, and this vortex may create localized melting zones in some areas of the interface. Such areas can be caused by internal heating based on the high pressure of explosive shock waves, intense plastic deformation, and heat generation due to the collapse of vortices in front of some wavefront due to the conversion of kinetic energy into thermal energy during a collision, and by the adiabatic heat caused by confined gases between the plates. These areas are surrounded by cold metal and are at a high cooling rate of 10^5-10^7 K / S [17].

The waveforms in the direction perpendicular to the explosion axis of the second sample are illustrated in Fig. 2b. It can be observed that the interface is a short wave in this case. As shown in Fig. 2c, the interface of the third series of samples is greater than that of the first series at the same standoff distance (3 mm) with local melting zones. The shape of the waves formed in the interface is asymmetric due to the differences in density and strength

between copper and 304 stainless steel. It can be seen that a certain amount of 304 stainless steel is pressed into the copper matrix, also the wave patterns incline along the direction of the explosion. This is primarily related to the significant differences between the thermophysical properties and mechanical properties of these couple plates. In front of the crest, there are some vortex regions, which were marked with red frames (as shown in Fig. 2c). There are an amount of fine equiaxed grains near the vortex regions in the copper matrix, exhibiting the characteristics of complete recrystallization. According to the EDS test results, it was determined that the vortex regions are a strong intermixing of copper and 304 stainless steel, which results from the circular movement and intense stirring following the propulsion process of explosive wave [17-18].

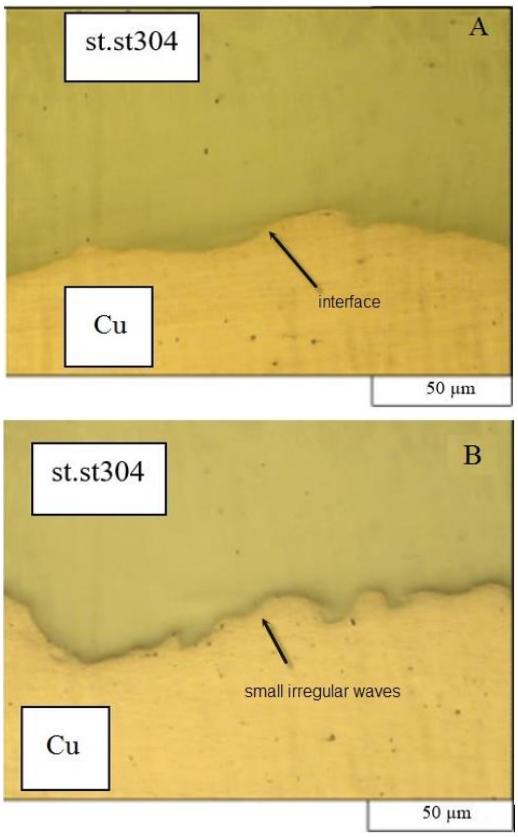

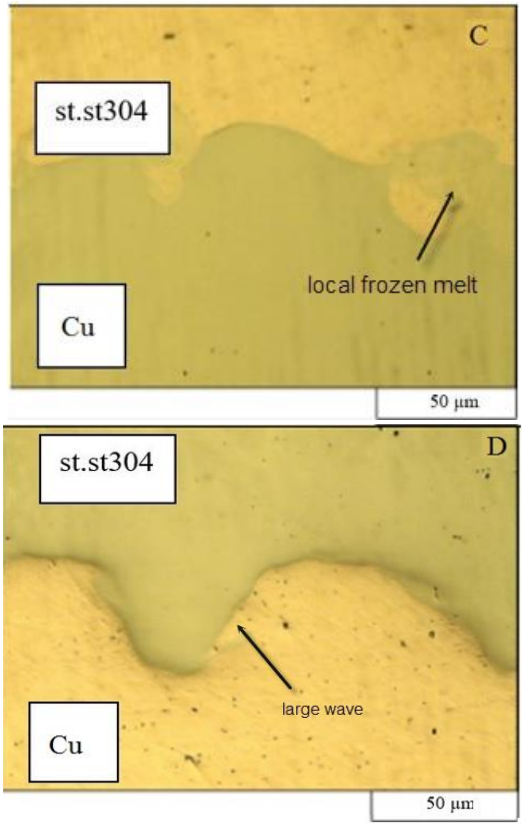

Fig. 2 OM images Interface A: The first specimen B: The second specimen C: The third specimen D: The fourth specimen.

In Fig. 2d, the interface of the fourth sample is shown with a standoff distance of 2 mm and an explosive thickness of 79 mm. As can be seen, the wavelength and height of the samples decreased compared to the third series due to the lower standoff distance, and it does not contain local melting zones.

The mechanism of the change of shape of the connection interface from a smooth to a wavy state in this research according to the connection variables and according to the research can be as follows, based on which the waves in front of the collision point are sunk by the relative velocity between the jumping crust. and the home page will be created. The creation of waves in front and behind the point of contact of the plates is due to the speed discontinuity in the common season, which occurs in both the descending and prominent jets relative to each other or to the plates, the change in the speed of the descending jet, which is from the plane Collider occurs, the main condition for the formation of a wave.

The difference in the current speed near the point of the impact causes a change in the wave pattern and the waveform can change quickly and the change from the sinusoidal state of the waveform is accelerated. The most recent studies conducted by Akbari Mousavi [18] also show that the speed discontinuity between the free surfaces of the welded plates is probably the cause of the wavy interface and the formation of waves due to the wave fluctuations of the materials and the change in the distribution of velocities on both sides of the interface.

3-2- Microstructure investigation of the samples by scanning electron microscopy

Fig. 3a shows the microscopic images of the first series. The interface, which is illustrated in this figure, is about 4 micrometers. The EDS analysis of the localized melting layer shows that the chemical composition of the interconnection consists of 18.1-12% iron, 81.88% copper, 1.93% nickel, and 1.24% chromium. The reason of appearing solidified interface zone is the combination of base plates and the flying plates as a result of forward jet rotation at the interface [19]. In Fig. 3, the images of the SEM represent the second sample with a standoff distance of 2 mm and an explosive charge of 63 mm. The reason for the increased interface thickness (25 μm) is the increase in explosive layer thickness and the higher kinetic energy of collision at the interface. In the EDS result, the composition of the local melting layer contains 20.94% iron, 68.26% copper, 3.50% nickel, and 7.30% chromium.

The SEM images of the interfacial sample of the third sample and the formation of the local melting layer are shown in Fig. 3c. In this sample, the thickness of the melting layer is greater than that of the fourth sample. According to the shape of the third series, the welding standoff distance is 3 mm, the explosive thickness is 79 mm. Due to the higher standoff distance, wave heights are greater than the fourth sample. The EDS analysis of the local melting layer indicated in Fig. 3c shows that the chemical composition of the local melting layer includes 18.36% iron, 73.17% copper, 41.2% atomic nickel, and 6.2% atom Chromium.

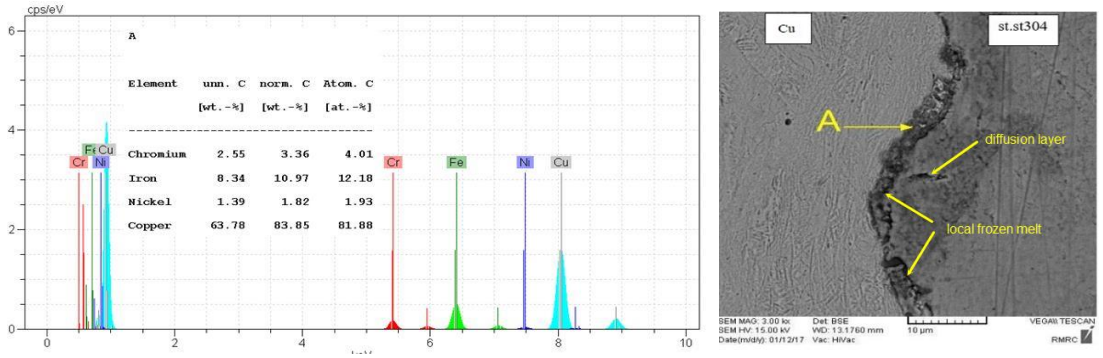

(A)

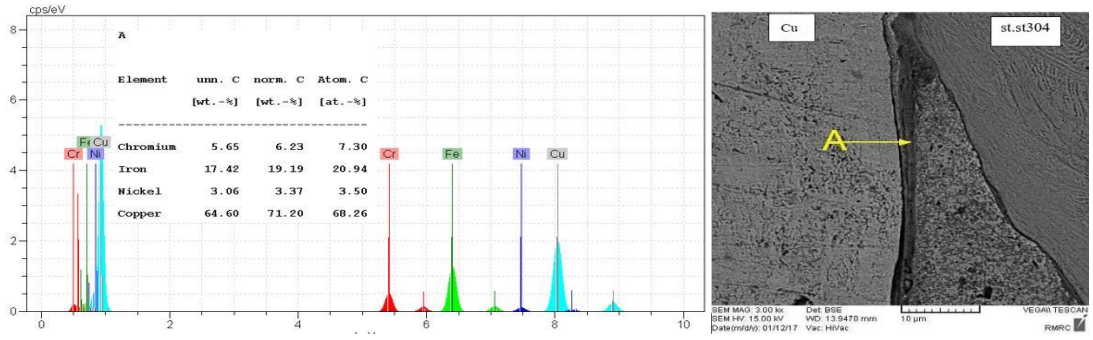

(B)

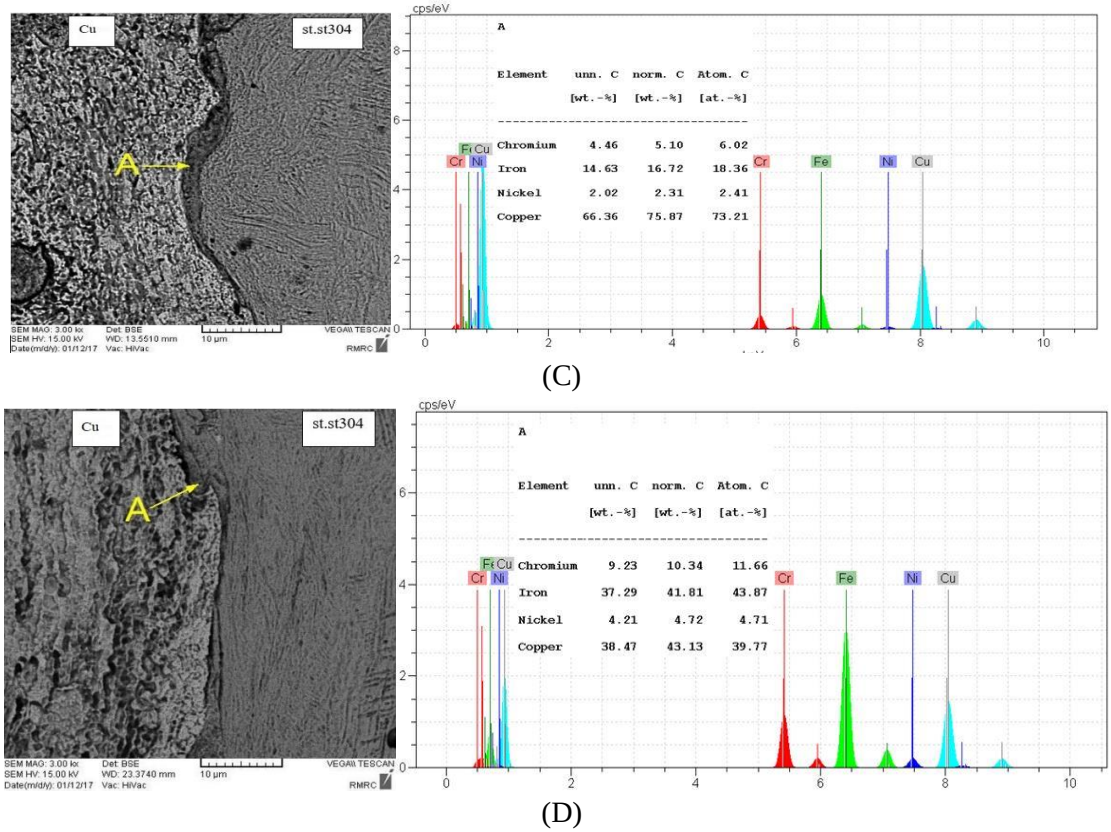

Fig. 3 SEM images and EDS analysis from the localized melting area at the connecting interface: A: The first example B: The second sample C: The third sample D: The fourth instance.

Fig. 3 shows the images of the SEM of the interface and the melting layer of the fourth series, with a standoff distance of 2 mm and an explosive layer thickness of 79 mm. In this sample, due to the low standoff distance and explosive thickness, the thickness of the melting layer is low. The composition of the structure consists of 43.87% iron, 39.77% copper, 4.71% nickel, and 11.66% chromium.

It was reported in the literature that in explosive welding, hard and brittle intermetallics would be formed during the welding process and these intermetallics affected the bonding quality in a negative manner [20]. From the Transmission Electron Microscope (TEM) bright field images, whether the diffusion layer or the melting layer, neither of them could be discovered the intermetallics distributing interior of the layers. That is because the solubility limit of copper in the g-iron is poor, the intermetallics can not be formed between iron and copper at the lower temperature. Consequently, the bonding quality will not be affected by this interface.

3-3- Micro-hardness testing results

In explosive welding, the flying and base plates are exposed to intense stress waves from explosives. These intense stress waves cause metallurgical changes and ultimately lead to an increase in microhardness. Microhardness is a function of chemical composition, percentage of alloy elements, intermetallic compounds, thermal changes, explosion charge, and standoff distance.

According to Table 3, the third sample has the highest hardness at the interface (HV 549) due to the high thickness of the explosive layer and the high standoff distance. The fourth and first samples have interface hardness of 532 and 516 HV respectively. Comparison between samples 1 and 3 shows that by increasing the thickness of the explosive from 46 mm to 79 mm, the hardness increases in the interface. The same results are obtained by comparing

samples 2 with 4. Compared to the results of samples 3 and 4, it can be concluded that with the increase in standoff distance, the measured hardness in the interface increases due to the increase of the standoff distance and explosive thickness, which leads to an increase in the velocity of flying plate and the dynamic angle of collision. As a result, collision kinetic energy increases, and more intense plastic deformation is caused in the interface area and the hardness achieved by explosive waves would be enhanced.

Table 3: Results of micro hardness (HV 0.05) from the joint phase of explosive samples

Sample number	standoff distance (mm)	Explosive Thickness (mm)	Micro hardness (HV 0.05) testing
1	3	46	516±2
2	2	63	501±1
3	3	79	549±1
4	2	79	532±3

3-4- Potentiodynamic Polarization results

The electrochemical parameters extracted from these curves, such as corrosion potential (E_{corr}), corrosion density (i_{corr}) (corrosion rate), and slopes of the anode and cathode Tafel, which are obtained using Tafel extrapolation are reported in Table 4.

In general, the parallel cathodic branches shown in Fig. 4 indicate that hydrogen propagation is controlled by activation, and the mechanism of H^+ ions reduction on the surface of the samples is not much affected by the welding operation. The anodic branches are different and are affected by various parameters of explosive welding. The results of Table 4 show that with the increase of standoff distance, the corrosion potential is reduced from -176 to -222 millivolts, and the corrosion density is increased from 0.53 to 0.86 microamperes per square centimeters. This is due to the increase in stored energy resulting from the collision caused by increased kinetic energy and standoff distance [21].

Table 4: Electrochemical parameters obtained from the polarization curves of the potentiodynamic were obtained from the explosive welding in a 3.5% NaCl solution at ambient temperature.

Sample number	standoff distance (mm)	Explosive Thickness (mm)	i_{corr} ($\mu A.m^{-2}$)	E_{corr} (mV)	β_a ($mV\,dec^{-1}$)	β_c ($mV\,dec^{-1}$)
1	3	46	7.47	-139	52	227
2	2	63	0.34	-200	48	75
3	3	79	0.86	-222	72	151
4	2	79	0.53	-176	52	195

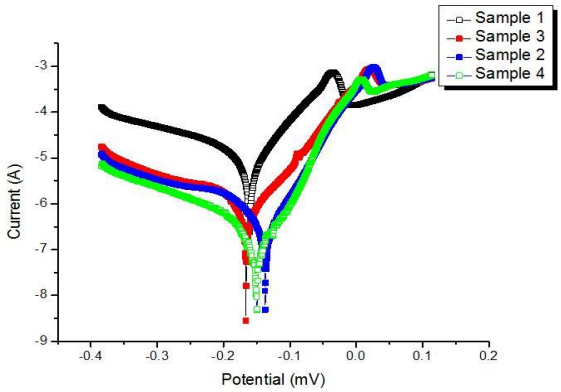

Fig. 4 Polarization behavior of explosive welding.

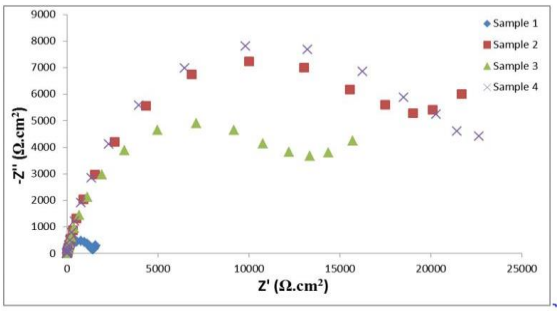

Fig. 5 Neuquist curves of samples from explosive welding

3-5- The results of electrochemical impedance spectroscopy

Electrochemical impedance spectroscopy (EIS) was used to study the surface layer created by the samples in a corrosive environment. The Nyquist diagrams of the explosive welding samples are shown in Fig. 5. EIS data are obtained using the equivalent circuit given in Fig. 6, which has an acceptable agreement with the empirical results, and are shown in Table 5.

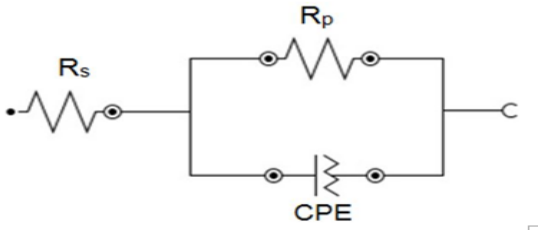

Fig. 6 Equivalent electric circuit diagram used to model the behavior of the metal / solvent interface.

Table 5: EIS data obtained from explosive welding in a 3.5% NaCl solution at ambient temperature

Sample number	standoff distance (mm)	Explosive Thickness (mm)	R_s (Ω)	R_p ($\Omega\,cm^2$)	C_{dl} ($\mu F\,cm^{-2}$)	n
1	3	46	18.3	1585	82.48	0.66
2	2	63	10.22	19810	29.57	0.81
3	3	79	10.9	13550	42.43	0.80
4	2	79	10.77	21300	31.73	0.82

From Fig. 5, it is observed that the obtained impedance loops in the Nyquist curve Have a slight deformation compared to a half-circle, which is known as a downward effect. In general, the deviation from the full half-circle is attributed to the frequency dispersion, as well as the surface heterogeneity and mass transfer resistance. This difference is described by the non-ideal behavior of a double-layer capacitor. Therefore, it seems necessary to use a constant phase element (CPE) instead of non-ideal double-layer capacitance behavior due to the distribution of relaxation times because of the heterogeneity of micro or Nano levels, such as roughness, porous layer, impurities, intrusive absorption, penetration and etc. in order to obtain more consistent results. The impedance of a constant phase element is expressed by the following equation:

$$Z_{CPE} = [Y_0(j\omega)^n]^{-1} \quad (1)$$

where Y_0 the Admittance and n are the uniformity coefficient of the surface (phase shift). If n is greater, the continuity and uniformity at the welding interface would be higher. For n = 0, 1, and 1, CPE indicates pure resistance behavior, pure net capacity, and pure induction respectively. [22].

In this study, the diameter of Neuquist curves is considered as the polarization resistance (R_p). In other words, only the existing capacity loops are related to the load transfer resistance between the metal and the outer Helmholtz layer (OHP). These observations indicate that metal corrosion is controlled by a load transfer process. The double electric layer can be described with the aid of an equivalent circuit and a good model of the metal / solvent interface. An equivalent electrical circuit for the samples in the solution is illustrated.

Fig. 7a by presenting a schematic model of potential distributions in the metal/solution interface (Fig. 7b) and the double-layer resistivity (Fig. 7c). In the presence of inhibitors, the polarization resistance (R_p) includes the load transfer resistance (R_{ct}), the resistance of the inhibitory layer on the metal surface (R_f), the accumulated alloys (inhibitory molecules, corrosion products, etc.) in the metal/solvent interface (R_a) and resistance of the inhibitor layer (R_d) $R_p = R_{ct} + R_f + R_{a+}R_d$ [21].

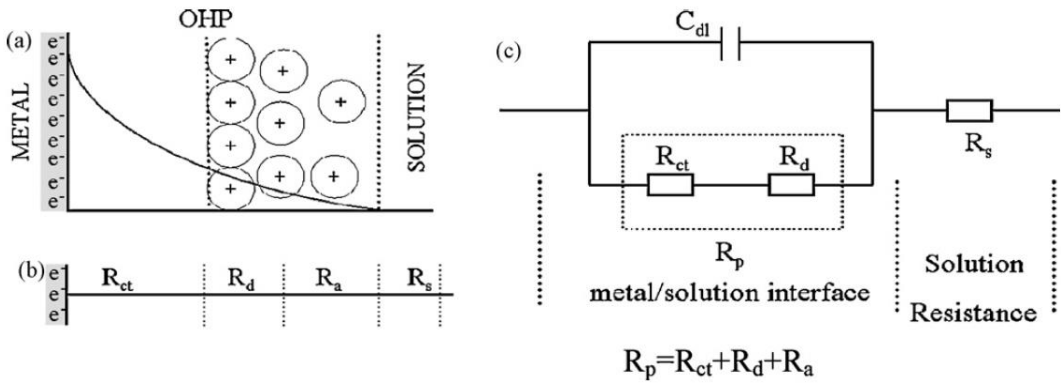

Fig. 7 Potential distributions in the metal / solution joint (a) dual layer resistance (b) and proposed electrical circuit for a non-inhibiting solution (c) [22].

The double-layer capacity C_{dl} is calculated using the following equation:

$$f(-Z''_{max}) = \frac{1}{2\pi C_{dl} R_{ct}} \quad (2)$$

where $-Z''_{max}$ is the maximum value of the imaginary part of the impedance? According to Table 4, sample 4 has the highest corrosion resistance (21300 ohms per square centimeter). In the next rank, sample 3 with a longer standoff distance has a polarization resistance of 13550 ohms per square centimeter. Finally, the first sample has the lowest polarization resistance. Besides, by comparing samples 1 and 3, it can be inferred that the number n increases with the increase of explosive thickness from 46 mm to 79 mm. The same result is obtained by comparing samples 2 and 4. Compared to the results of samples 3 and 4, it can be concluded that with the increase of standoff distance, the measured number n decreases due to standoff distance and explosive

thickness augmentation, which leads to an increase in the velocity of the flying plate and the dynamic angle. As a result, the kinetic energy of the collision increases, and more plastic deformation is caused. Moreover, according to the local melting zones in samples 3 and 4, it can be concluded that by increasing the standoff distance, the amount of copper available in these areas increased, which led to the increased corrosion rate of the galvanic cell.

4- Conclusion

In this study, an investigation of corrosion behavior and microstructural variations of the explosive welding of copper-304 stainless steel sheets by explosive welding process along with standoff distance and explosive thickness was carried out, and the following results were obtained:

1. The morphology of the joint surface is different under different explosive welding parameters, and regular wave bonding can occur for larger explosive ratio.

2. Microstructure observations revealed that the microstructure of the bonding interface presented a nearly straight interface, periodic wavy interface and irregularly wave interface along the detonation direction, which corresponded to the growth zone, steady zone and reflection-affected zone of the detonation wave. The periodic wavy bonding structure with both vortex region and solid-solid bonding region was embedded in the interface.

3. Microhardness studies showed an increase in hardness value with increasing standoff distance and explosive thickness, which was mainly due to high impact pressure and severe plastic deformation in the weld zone. Sample 3 with large wave morphology showed the highest microhardness value (549±1 HV) among all samples.

4. According to the results of the corrosion test, the resistance to corrosion increases with the increase of the standoff distance and explosive thickness. Sample 4 has the highest corrosion resistance and its value is equal to 21300 Ωcm^2, and the first sample has the lowest value (1585 Ωcm^2) of polarization resistance.

5. Also, according to the results of the corrosion test in samples 3 and 4, it can be concluded that with the increase in the standoff distance, the amount of copper in the local frozen melt of these samples has increased, which increases the severity of corrosion caused by the galvanic cell.

References

[1] Paul, H., Petrzak, P., Chulist, R., Maj, L. And Mania, I. (2022). Effect of impact loading and heat treatment on microstructure and properties of multi-layered AZ31/AA1050 plates fabricated by single-shot explosive welding. Materials and Design. 214: 1-19.

[2] Atifeh, S.M., Rouzbeh, A. and Hashemi, R. 2022. Effect of Annealing on Formability and Mechanical Properties of AA1050/Mg-AZ31B Bilayer Sheets Fabricated by Explosive Welding Method. The International Journal of Advanced Manufacturing Technology. 118: 775–784

[3] Shi, Y., Wang, J., Zhou, X. and Xue, x. (2023). Post–Fire Properties of Stainless–Clad Bimetallic Steel Produced by Explosive Welding Process. Journal of Constructional Steel Research. 201: 2-17.

[4] Zhou, Q., Liu, R., Zhou, Q., Ran, C., Fan, K., Xie, J. and Chen, p. (2022). Effect of Microstructure on Mechanical Properties of Titanium-Steel Explosive Welding Interface. Materials Science & Engineering A. 830: 1-12.

[5] Yazdani, A., Naseri, R. and Rahmati, S. (2017). Investigation of Pringback of Two-Layer Metallic Sheet Produced by Explosive Welding in U-die Bending Process. *J* Journal of Engg. Research. 5: 187-206.

[6] Durgutlu, A., Gulenc, B. and Findik, F. Examination of copper/stainless steel joints formed by explosive welding. Materials and Design. 26: 497-507.

[7] Durgutlu, A., Okuyucu, H. and Gulenc, B. (2008). Investigation of Effect of the Stand-off Distance on Interface Characteristics of Explosively

Welded Copper and Stainless Steel. Materials and Design. 29: 1480-1484.

[8] Langeslag, S. A. E., Sgobba, S., Libeyre, P. and Gung, C.-Y. (2015). Extensive Characterisation of Copper-clad Plates, Bonded by the Explosive Technique, for ITER Electrical Joints. Physics Procedia. 67: 1036-1042.

[9] Kahraman, N. and G¨ulenc, B. (2007). Corrosion and Mechanical-Microstructural Aspects of Dissimilar Joints of Ti–6Al–4V and Al Plates. International Journal of Impact Engineering. 34: 1423–1432.

[10] Kahraman, N. and G¨ulenc B. (2005). Joining of Titanium/Stainless Steel by Explosive Welding and Effect on Interface. Journal of Materials Processing Technology. 169: 127–133.

[11] Kengkla, N. and Tareelap, N. (2012). Role of intermetallic compound on crrosion of aluminium/steel transition joint used in naval applications. 1st Mae Fah Luang University International Conference.

[12] Acarer, M. Electrical, Corrosion, and Mechanical Properties of Aluminum-Copper Joints Produced by Explosive Welding. Materials Engineering and Performa. 21: 2375-2379.

[13] Kamachi Mudali, U., Ananda Rao, B. M., Shanmugam, K., Natarajan, R. and Raj, B. (2003). Corrosion and Microstructural Aspects of Dissimilar Joints of Titanium and Type 304L Stainless Steel Journal of Nuclear Materials. 321: 40–48.

[14] Stansbury, E. E. and Buchanan, R. A. (2000). Fundamentals of Electrochemical Corrosion, ASM International.

[15] Verma, J. and Vasantrao Taiwade, R. (2016). Dissimilar Welding Behavior of 22% Cr Series Stainless Steel with 316L and its Corrosion Resistance in Modified Aggressive Environment Journal of Manufacturing Processes. 24: 1–10.

[16] Potesser, M. and Schoeberl, T. (2006). The characterization of the intermetallic fe-al layer of steel-aluminumweldings. TMS, The Minerals, Metals & Materials Society.

[17] Crossland, B. Explosive Welding of Metals and its Applications. Oxford Science Publication.

[18] Akbari Mousavi S.A.A. and farhadi sartangi P. 2008. Effect of Post-Weld Heat Treatment on the Interface Microstructure of Explosively Welded Titanium-Stainless Steel Composite. Material science and engineering A. 494: 329-336.

[19] Padash, E., Khanzadeh, M. R., Bakhtiari, H., Bakhtiari, Z., Shajari, Y. and Seyedraoufi, Z. (2021). Effect of Heat Treatment Duration on Interface Characteristics of Explosively Bonded Cu/SS-304 Plates. Metallography, Microstructure, and Analysis. 10: 74-85.

[20] Wu T. and Yang C. (2022). Influence of Pulse TIG Welding Thermal Cycling on the Microstructure and Mechanical Properties of Explosively Weld Titanium/Steel Joint. Vacuum. 197: 1-16.

[21] Kahraman, N. and G¨ulenc, B. (2005). Joining of Titanium/Stainless Steel by Explosive Welding and Effect on Interface. Journal of Materials Processing Technology. 169: 127–133.

[22] Kahraman, N. and G¨ulenc, B. (2007). Corrosion and Mechanical-Microstructural Aspects of Dissimilar Joints of Ti–6Al–4V and Al Plates. International Journal of Impact Engineering. 34: 1423–1432.